GEOPHYSICS, VOL. 60, NO. 5 (SEPTEMBER-OCTOBER 1995); P. 1550–1566, 21 FIGS.

Velocity analysis for transversely isotropic media

Tariq Alkhalifah* and Ilya Tsvankin*

ABSTRACT

The main difficulty in extending seismic processing to anisotropic media is the recovery of anisotropic velocity fields from surface reflection data. We suggest carrying out velocity analysis for transversely isotropic (TI) media by inverting the dependence of *P*-wave moveout velocities on the ray parameter. The inversion technique is based on the exact analytic equation for the normal-moveout (NMO) velocity for dipping reflectors in anisotropic media.

We show that *P*-wave NMO velocity for dipping reflectors in homogeneous TI media with a vertical symmetry axis depends just on the zero-dip value $V_{\rm nmo}(0)$ and a new effective parameter η that reduces to the difference between Thomsen parameters ε and δ in the limit of weak anisotropy. Our inversion procedure makes it possible to obtain η and reconstruct the NMO velocity as a function of ray parameter using moveout velocities for two different dips. Moreover, $V_{\rm nmo}(0)$ and η determine not only the NMO velocity, but also long-spread (nonhyperbolic) *P*-wave moveout for horizontal reflectors and the time-migration impulse response. This means that inversion of dip-moveout information allows one to perform all time-processing steps in TI media using only surface *P*-wave data. For elliptical anisotropy ($\varepsilon = \delta$), isotropic time-processing methods remain entirely valid. We show the performance of our velocity-analysis method not only on synthetic, but also on field data from offshore Africa.

Accurate time-to-depth conversion, however, requires that the vertical velocity V_{P0} be resolved independently. Unfortunately, it cannot be done using *P*-wave surface moveout data alone, no matter how many dips are available. In some cases V_{P0} is known (e.g., from check shots or well logs); then the anisotropy parameters ε and δ can be found by inverting two *P*-wave NMO velocities corresponding to a horizontal and a dipping reflector. If no well information is available, all three parameters (V_{P0}, ε, and δ) can be obtained by combining our inversion results with shear-wave information, such as the *P-SV* or *SV-SV* wave NMO velocities for a horizontal reflector.

Generalization of the single-layer NMO equation to layered anisotropic media with a dipping reflector provides a basis for extending anisotropic velocity analysis to vertically inhomogeneous media. We demonstrate how the influence of a stratified anisotropic overburden on moveout velocity can be stripped through a Dix-type differentiation procedure.

INTRODUCTION

The importance of anisotropic phenomena in wave propagation and processing of seismic data is now widely recognized by the exploration community. Progress in accounting for anisotropy in seismic processing, however, has been slow, mostly as a result of the difficulty in obtaining anisotropic velocity fields from surface seismic data. For instance, there exist a number of migration algorithms for transversely isotropic media (VerWest, 1989; Sena and Toksöz, 1993; Alkhalifah, 1995), but their application requires knowledge of the anisotropic velocity model. Clearly, the recovery of several independent elastic coefficients needed to reconstruct the anisotropic velocity function is much more complicated than is conventional velocity analysis for isotropic media, especially because of the limited angle coverage of reflection surveys.

Existing work on anisotropic traveltime inversion of reflection data has been done for laterally homogeneous subsurface models (Byun and Corrigan, 1990; Sena, 1991; Tsvankin and Thomsen, 1995). As shown in Tsvankin and Thomsen (1995), *P*-wave moveout from horizontal reflectors is insufficient to recover the parameters of transversely isotropic media with a vertical symmetry axis (VTI), even if

Manuscript received by the Editor August 31, 1994; revised manuscript received December 12, 1994.
*Center for Wave Phenomena, Colorado School of Mines, Golden, CO 80401-1887.

long spreads (twice the reflector depth) are used. The reason for this ambiguity is the trade-off between the vertical velocity and anisotropic coefficients, which cannot be overcome even by using the nonhyperbolic portion of the moveout curve. Tsvankin and Thomsen (1995) conclude that the only way to carry out stable inversion of surface reflection data is to combine long-spread P and SV moveouts; however, this method encounters many practical difficulties. Therefore, to make the anisotropic inversion feasible, P-wave reflection moveout in laterally homogeneous media should be supplemented by additional information (e.g., the vertical velocity from check shots or well logs).

The presence of dipping reflectors provides us with the opportunity of extending the angle coverage of the input data without using nonhyperbolic moveout. Here, we develop an inversion technique for transversely isotropic media based on the analytic equation for normal moveout (NMO) velocity for dipping reflectors derived by Tsvankin (1995). We recast this equation as a function of ray parameter and use it in inverting dip-dependent P-wave NMO velocities for the anisotropic coefficients. Analysis of the stability of the inverse problem by means of the Jacobian matrix is followed by the actual numerical inversion procedure via the Newton-Raphson method. We show that this approach makes it possible to obtain a family of solutions that all have the same NMO velocity for all possible dips, as well as the same nonhyperbolic moveout for horizontal reflectors, and the same time-migration impulse response. This family of solutions is described fully just by two parameters: the NMO velocity for a horizontal reflector and a new anisotropic coefficient that we denote as η. Then, we extend our results to vertically inhomogeneous anisotropic media by developing a Dix-type procedure (Dix, 1955) intended to give estimates of the NMO velocity in any individual layer from surface reflection data. We conclude by showing an application of our method to a marine data set from offshore Africa.

NMO VELOCITY FOR DIPPING REFLECTORS IN TI MEDIA

Our analysis is based on the equation for the normal-moveout (short-spread) velocity for dipping reflectors in a homogeneous anisotropic medium derived in Tsvankin (1995):

$$V_{\mathrm{nmo}}(\phi) = \frac{V(\phi)}{\cos\phi}\,\frac{\sqrt{1+\dfrac{1}{V(\phi)}\dfrac{d^2V}{d\theta^2}}}{1-\dfrac{\tan\phi}{V(\phi)}\dfrac{dV}{d\theta}}, \qquad (1)$$

where V is the phase velocity as a function of the phase angle θ (θ is measured from vertical) and ϕ is the dip angle of the reflector; the derivatives are evaluated at the dip ϕ.

Formula (1) is valid in symmetry planes of any anisotropic medium and is not restricted to any particular wave type. It assumes, however, that the incidence (sagittal) plane is the dip plane of the reflector. Here we will use this equation only for P-waves in VTI media.

The NMO velocity [equation (1)] is a function of phase velocity $V(\theta)$ and its first two derivatives taken at the dip ϕ. Unfortunately, reflection data do not carry any explicit information about the dip; rather, we can count on recovering the ray parameter $p(\phi)$ corresponding to the zero-offset reflection.

$$p(\phi) = \frac{1}{2}\frac{dt_0}{dx_0} = \frac{\sin\phi}{V(\phi)}, \qquad (2)$$

where $t_0(x_0)$ is the two-way traveltime on the zero-offset (or stacked) section, and x_0 is the midpoint position.

In the numerical analysis of the NMO velocity, the replacement of the angle ϕ by the ray parameter p (horizontal slowness) does not pose any serious problem. Phase velocity and phase angle can be found from the Christoffel equations in a straightforward fashion if horizontal slowness is known, as shown in Appendix A. At the same time, the substitution of p may change the influence of the elastic coefficients on the NMO velocity since the form of the equation will change.

In conventional notation, P-wave propagation in transversely isotropic models is described by four stiffness coefficients: c_{11}, c_{33}, c_{13}, and c_{44}. The number of independent parameters, however, can be reduced by using the notation suggested in Thomsen (1986). Formally, P-wave phase and group velocity depend on four Thomsen parameters: P- and S-wave vertical velocities V_{P0} and V_{S0} and the dimensionless anisotropy parameters ε and δ defined as

$$\varepsilon \equiv \frac{c_{11}-c_{33}}{2c_{33}} \qquad (3)$$

and

$$\delta \equiv \frac{(c_{13}+c_{44})^2-(c_{33}-c_{44})^2}{2c_{33}(c_{33}-c_{44})}. \qquad (4)$$

However, the influence of the shear-wave vertical velocity on P-wave velocities and traveltimes is practically negligible, even for strong anisotropy (Tsvankin and Thomsen, 1994; Alkhalifah and Larner, 1994). In an overview paper (P-wave signatures and notation for transversely isotropic media: An overview, accepted for Geophysics, 1996), shows that for most practical purposes the influence of V_{S0} on all P-wave kinematic signatures, including moveout velocity V_{nmo}, can be ignored. Therefore, in our inversion procedure we will attempt to recover only the parameters V_{P0}, ε, and δ.

For a horizontal reflector, equation (1) reduces to the well-known formula for NMO velocity (Thomsen, 1986):

$$V_{\mathrm{nmo}}(0) = V_{P0}\sqrt{1+2\delta}. \qquad (5)$$

The trade-off between the vertical velocity V_{P0} and parameter δ cannot be resolved even if the NMO velocities for all three (P, SV, and SH) waves from a horizontal reflector are known (Tsvankin and Thomsen, 1995). On the other hand, if V_{P0} is known (e.g., from check shots or well logs), the zero-dip moveout velocity [equation (5)] can be used to obtain δ.

Analytic and numerical analysis performed by Tsvankin (1995) shows that the dip-dependence of P-wave NMO velocities is mostly controlled by the difference between ε and δ. Therefore, if δ has been determined from $V_{\mathrm{nmo}}(0)$, we should be able to find ε from a single NMO velocity for a dipping reflector. It is also interesting to examine the possibility of recovering all three parameters (V_{P0}, ε, and δ) from

NMO velocities at three (or more) distinct dips. This analysis is performed numerically in the next sections.

NMO VELOCITY FOR ELLIPTICAL AND WEAK ANISOTROPY

Before proceeding with the numerical inversion procedure, we will elucidate the peculiarities of equation (1) by considering the special cases of elliptical and weak anisotropy. Unfortunately, NMO equation (1) is too complex to allow for analytic insight into the contributions of the anisotropic coefficients for general transverse isotropy.

For elliptical anisotropy ($\varepsilon = \delta$), the NMO velocity as a function of ray parameter is given by (Appendix A)

$$V_{\rm nmo}(p) = \frac{V_{\rm nmo}(0)}{\sqrt{1 - p^2 V_{\rm nmo}^2(0)}}. \qquad (6)$$

Equation (6) is a good illustration of the difference between the NMO equations expressed through the dip angle and ray parameter. Tsvankin (1995) shows that if the dip ϕ is used as the argument, the distortion in the NMO velocity caused by elliptical anisotropy is proportional to the ratio of the phase velocities $V(\phi)/V(0) = \sqrt{1 + 2\delta \sin^2 \phi}$. Therefore, $V_{\rm nmo}(\phi)$ contains a separate contribution of the parameter δ. However, $V_{\rm nmo}$ expressed through ray parameter [equation (6)] is a function just of the zero-dip NMO velocity with no separate dependence on the vertical velocity or on δ. In fact, equation (6) coincides with the NMO formula for isotropic media; the influence of the anisotropy in formula (6) is absorbed by the value of $V_{\rm nmo}(0)$, given by equation (5). This was discussed in Tsvankin (1995) in the section devoted to the so-called "apparent" dip angle $\hat{\phi}$ ($\sin \hat{\phi} = pV_{\rm nmo}(0)$).

In terms of the inversion procedure, this result means that for elliptical models, the trade-off between V_{P0} and δ in equation (5) cannot be resolved from the dip-dependence of P-wave NMO velocity [equation (6)]. Moreover, the reflection moveout for elliptical anisotropy is purely hyperbolic and does not provide any information other than the zero-dip NMO (short-spread) velocity [equation (5)], which is identical (for a vertical symmetry axis) to the horizontal velocity of the medium. On the other hand, the NMO velocity as a function of p can be easily reconstructed from the NMO velocity for a horizontal reflector; this conclusion has important implications in dip-moveout processing.

To understand the behavior of $V_{\rm nmo}(p)$ for nonelliptical models, we use the weak-anisotropy approximation ($|\varepsilon| \ll 1$, $|\delta| \ll 1$). Equation (1) as a function of ray parameter for weak transverse isotropy is derived in Appendix A:

$$V_{\rm nmo}(p) = \frac{V_{\rm nmo}(0)}{\sqrt{1 - y}} [1 + (\varepsilon - \delta) f(y)], \qquad (7)$$

where

$$f(y) = \frac{y(4y^2 - 9y + 6)}{1 - y}, \quad y \equiv p^2 V_{\rm nmo}^2(0).$$

Note that for elliptical anisotropy, the weak-anisotropy approximation [equation (7)] reduces to the exact NMO equation (6).

Again, it is interesting to compare equation (7) with the corresponding weak-anisotropy NMO equation as a function of the dip angle, given in Tsvankin (1995). Although Tsvankin (1995) emphasized the difference $\varepsilon - \delta$ as the most influential parameter in his NMO equation, $V_{\rm nmo}(\phi)$ does contain a separate contribution of δ. However, when the dip angle is replaced by the ray parameter, the NMO velocity explicitly contains the anisotropy parameters only in the form of the combination $\varepsilon - \delta$. Of course, δ is also hidden in the value of $V_{\rm nmo}(0)$.

This result has important implications in the inversion procedure. Instead of the three original unknown parameters (V_{P0}, ε, and δ), in the limit of weak anisotropy, the NMO velocity contains just two combinations of them—$V_{\rm nmo}(0)$ and $\varepsilon - \delta$. Therefore, moveout (stacking) velocities from just two distinct dips should provide enough information to recover the two effective parameters and reconstruct the NMO velocity as a function of ray parameter. In the most common case, when the zero-dip NMO velocity has been found by conventional NMO analysis, a single additional dipping reflector makes it possible to recover the difference $\varepsilon - \delta$. However, the trade-off between V_{P0}, ε, and δ cannot be resolved from P-wave NMO velocities for weak transverse isotropy, no matter how many reflectors (dips) are used. Normal moveout velocities from more than two dipping reflectors just provide redundancy in the estimation of $V_{\rm nmo}(0)$ and the difference $\varepsilon - \delta$.

Although these conclusions have been drawn for weak transverse isotropy, the numerical analysis in the following sections leads to similar results for VTI media with arbitrary strength of the anisotropy.

CONDITIONING OF THE PROBLEM

To estimate the sensitivity of the NMO velocity to the anisotropic parameters, we evaluate the Jacobian of equation (1) expressed as a function of ray parameter. The Jacobian is obtained by calculating the derivatives of the NMO velocity equation with respect to the model parameters V_{P0}, ε, and δ. First, we consider the case of inverting for two parameters (namely, ε and δ) using two different dips; next, we examine the inversion for all three parameters.

Although the NMO velocity equation is nonlinear, its dependence on the anisotropy parameters is smooth enough to use the Jacobian approximation. Figure 1 is a 3-D plot of the values of $V_{\rm nmo}$ as a function of ε and δ for a reflector dip of nearly 40° (for a given p, the dip changes somewhat with ε and δ) and a vertical velocity V_{P0} of 3.0 km/s. The smoothness of equation (1) over a practical range of ε and δ is evident.

The derivatives used to form the Jacobian are as follows:

$$d_1(p) = \frac{V_{P0}}{V_{\rm nmo}(p)} \frac{\partial V_{\rm nmo}(p)}{\partial V_{P0}},$$

$$d_2(p) = \frac{1}{V_{\rm nmo}(p)} \frac{\partial V_{\rm nmo}(p)}{\partial \delta},$$

$$d_3(p) = \frac{1}{V_{\rm nmo}(p)} \frac{\partial V_{\rm nmo}(p)}{\partial \varepsilon}.$$

We calculate d_1, d_2, and d_3 numerically using equation (1). The normalization of the derivatives makes them easier to use. For example, $d_3 = 1$ implies that, when solving only for ε, a 5% error in the measured NMO velocity would cause an error of 0.05 in the calculated value of ε.

If two distinct reflector dips are available, it may be possible to solve for two of the three parameters. The sensitivity of this inversion to errors in the input data (NMO velocities) can be measured from the Jacobian matrix,

$$\mathbf{J} = \begin{pmatrix} d_2(p_1) & d_3(p_1) \\ d_2(p_2) & d_3(p_2) \end{pmatrix}.$$

This Jacobian corresponds to the inversion for ε and δ when V_{P0} is known.

The condition number κ for Jacobian matrix J can be computed as follows:

$$\kappa = \sqrt{\frac{|\lambda_{\max}|}{|\lambda_{\min}|}},$$

where $\lambda_{\max}$ and $\lambda_{\min}$ are the maximum and minimum eigenvalues, respectively, of the matrix

$$A = JJ^T.$$

J^T is the transpose of the matrix $\mathbf{J}$. A large condition number implies an ill-conditioned (i.e., nearly singular) problem, while a low condition number (for example, smaller than 10) usually implies a well-conditioned problem. The absolute errors in the computed anisotropy parameters and the relative error in the computed V_{P0} are close to κ times the relative error in the measured NMO velocity. In most cases, this estimate provides the maximum possible error.

Figure 2 shows the condition number as a function of ray parameter for the inversion of the NMO velocities measured at two dips, corresponding to p_1 and p_2. The dips range from 0 to 60°. The flat (clipped) parts of the 3-D plot correspond to high condition numbers ($\geq$6.0). When the dips are close to each other, the problem becomes highly ill-conditioned (i.e., the diagonal line where $p_1 = p_2$). If the difference between the dips is 10–15° or more, the problem becomes reasonably conditioned, unless both dip angles are large (>25°). The latter case, however, is hardly typical. In a typical case of horizontal and dipping reflectors, an acceptable resolution in resolving ε and δ is achieved (for the model from Figure 2) for a wide range of ray parameters that excludes only those values corresponding to mild dips.

The inversion for the important case of a horizontal and a dipping reflector needs to be considered in more detail. Figure 3 shows the condition number for the inversion for ε and δ (V_{P0} is considered to be known), with reflector dips given by $p_1 = 0.0$ (horizontal reflector) and $p_2 = 0.16$ (near 30° dip). The low values of the condition number mean that overall we obtain a reasonably good resolution over a wide range of values of ε and δ.

Next, we examine the feasibility of inverting for all three parameters (V_{P0}, ε, and δ) using NMO velocities for three different dips. The Jacobian matrix for this problem is

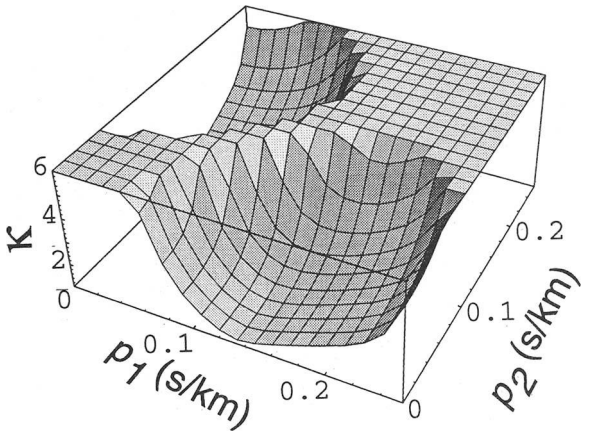

FIG. 2. A 3-D plot of the condition number as a function of p_1 and p_2 (ray parameters of the two reflectors). The model parameters are $V_{P0} = 3.0$ km/s, $\varepsilon = 0.2$, and $\delta = 0.1$.

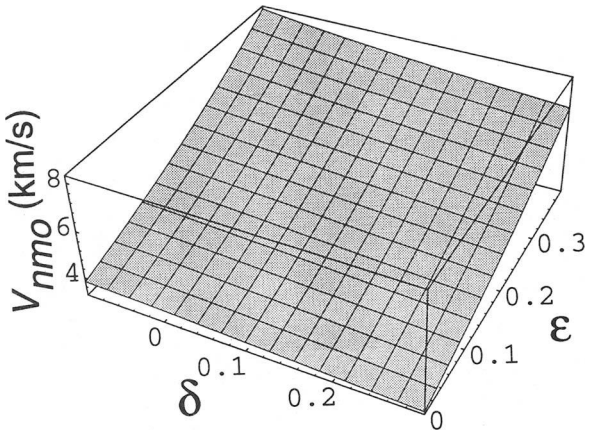

FIG. 1. A 3-D plot of the NMO velocity as a function of ε and δ for the reflector dip corresponding to $p = 0.2$ s/km; $V_{P0} = 3.0$ km/s.

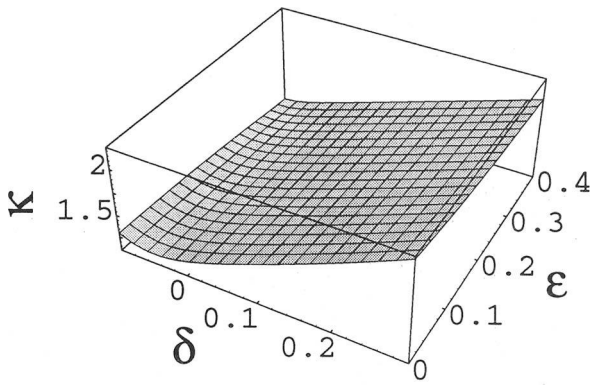

FIG. 3. A 3-D plot of the condition number as a function of ε and δ. Two reflector dips used in the inversion correspond to ray parameters of $p_1 = 0.0$ s/km (horizontal reflector) and $p_2 = 0.16$ s/km. The vertical velocity V_{P0} is 3.0 km/s.

$$\mathbf{J} = \begin{pmatrix} d_1(p_1) & d_2(p_1) & d_3(p_1) \\ d_1(p_2) & d_2(p_2) & d_3(p_2) \\ d_1(p_3) & d_2(p_3) & d_3(p_3) \end{pmatrix}. \quad (8)$$

Figure 4 shows the condition number for the Jacobian (8) calculated for reflector dips $p_1 = 0.0$ (horizontal reflector), $p_2 = 0.16$ s/km (near 30° dip), and $p_3 = 0.23$ s/km (near 50° dip). The huge values of the condition number over the entire range of ε indicate that the problem is thoroughly ill-posed. In other words, we could find models with a wide range of V_{P0}, ε, and δ that have almost the same NMO velocities for the dips considered here. This ill-conditioned nature holds for all choices of ray parameters, V_{P0}, ε, and δ that we have studied.

Note that for models close to elliptical ($\varepsilon = \delta$), the condition number goes to infinity, and the inversion cannot be carried out at all. Above, we obtained this result analytically by showing that the NMO equation for elliptical anisotropy (6) depends only on the ray parameter and the zero-dip NMO velocity.

Given the uncertainties usually associated with seismic data, we cannot count on resolving all three parameters using this method, even if we had more than three different reflector dips. The ambiguity of the inversion procedure is caused by the trade-off between the anisotropy parameters ε and δ in the NMO equation. In the limit of weak anisotropy, this trade-off is demonstrated by the NMO formula (7), which contains only the *difference* $\varepsilon - \delta$ and the zero-dip NMO velocity rather than either of the coefficients individually. However, as we have seen, if one of the parameters (V_{P0}, ε, δ) is known, the other two can be reliably recovered from NMO velocities for two different dips.

NUMERICAL INVERSION

The above analysis based on the Jacobian matrix is still approximate since the NMO velocity equation is nonlinear. In this section, we perform the actual nonlinear inversion by means of the Newton-Raphson method and study the range of solutions as well as the sensitivity of the results to errors in the input information. We will concentrate on models with $\varepsilon - \delta \geq 0$, which are believed to be most typical for subsurface formations (Thomsen, 1986; Tsvankin and Thomsen, 1994).

Inversion using two reflector dips

The input data for the inversion procedure are the P-wave NMO velocities and ray parameters for two different reflector dips; one of the reflectors can be (but is not necessarily) horizontal. For conventional spreadlengths, limited by the distance between the common midpoint (CMP) and the reflector, NMO velocity is well-approximated by the stacking velocity routinely used in seismic processing (Tsvankin and Thomsen, 1994; Tsvankin, 1995). The analysis in the previous section indicates that the inversion for all three parameters using three reflector dips is unstable; besides, for our method to be practical we can seldom count on having reliable NMO velocities from more than two distinctly different dips.

The convergence of the inversion procedure is related to the value of the condition number examined in the previous section. As illustrated in Figure 2, the condition number is low for a wide range of dips, except for those close to each other. This implies good convergence properties of the inversion procedure, provided we pick a plausible initial model. In our implementation, we used the isotropic model ($\delta = \varepsilon = 0$) as the initial guess and achieved a fast convergence in the numerical examples described below.

In our first example (Figure 5), we consider a horizontal reflector and a reflector dipping at 50° ($p = 0.23$ s/km) for the same model as in Figure 2 ($V_{P0} = 3.0$ km/s, $\varepsilon = 0.2$, and $\delta = 0.1$).

If we know the vertical velocity V_{P0}, the inversion of two NMO velocities should make it possible to recover ε and δ. Indeed, as shown in Figure 5, if the actual velocity $V_{P0} = 3.0$ km/s is used in the Newton-Raphson inversion algorithm, we obtain the correct values for both anisotropic parameters.

If only surface data are available, however, the exact vertical velocity may not be known. Therefore, it is inter-

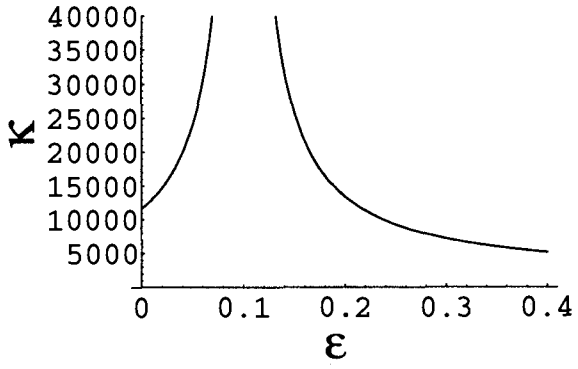

FIG. 4. Condition number as a function of ε for the inversion using three reflector dips corresponding to $p_1 = 0.0$ s/km, $p_2 = 0.16$ s/km, and $p_3 = 0.23$ s/km. The vertical velocity is $V_{P0} = 3.0$ km/s; $\delta = 0.1$.

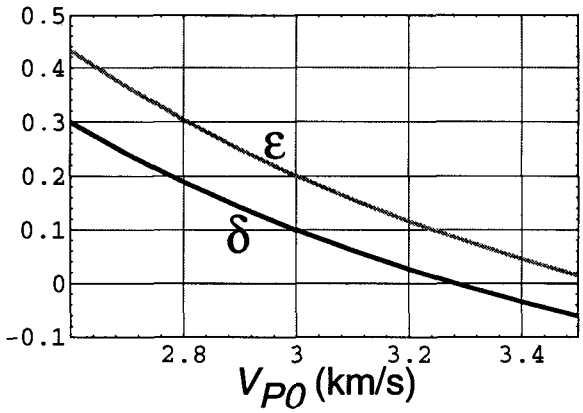

FIG. 5. Parameters ε and δ obtained from NMO velocities corresponding to a horizontal reflector and $p = 0.23$ s/km (50° dip). The values of V_{P0} used in the inversion are shown on the horizontal axis. The model parameters are $V_{P0} = 3.0$ km/s, $\varepsilon = 0.2$, and $\delta = 0.1$.

esting to examine the family of solutions corresponding to a range of vertical velocities around the actual value (from 2.6 km/s to 3.5 km/s in Figure 5). For all these solutions, the difference between ε and δ is close to the exact value ($\varepsilon - \delta = 0.1$). Therefore, in remarkable agreement with the weak-anisotropy approximation [equation (7)], the inversion of the *P*-wave NMO velocities provides us with a good estimate of the difference $\varepsilon - \delta$. The only way to resolve the coefficients individually is to obtain the vertical velocity V_{P0} using some other source of information (e.g., check shots or well logs).

The most important property of the family of solutions shown in Figure 5 is that all of them have practically the same NMO velocity as a function of ray parameter for all possible dipping reflectors, not just for the two dips used in the inversion scheme. This is illustrated in Figure 6, which shows that the NMO velocity for any given reflector dip (i.e., any fixed value of p) is practically the same within the range of solutions in Figure 5, independent of the guess for V_{P0}. Therefore, if we perform the inversion procedure using the NMO velocities for any two dipping reflectors (of course, the dips should not be close to each other), we end up with the same family of equivalent models as in Figure 5. In the following, we refer to models obtained by the inversion of *P*-wave NMO velocity as the "equivalent solutions," or ES.

We conclude that the normal moveout velocities measured at two different dips are sufficient to obtain the NMO velocity for any ray-parameter value. This means that the dip-dependent *P*-wave NMO velocity is controlled by just two combinations of the parameters V_{P0}, ε, and δ, rather than by the three parameters individually.

Another example, for a medium with stronger anisotropy, is shown in Figure 7. Here, we have considered a typical case of horizontal and dipping reflectors (the dip angle is 40°); it should be emphasized that any pair of dips sufficiently different from each other yields the same family of ES. Thus, as for the previous model, all ES have the same NMO velocity for the full range of dips. However, in contrast with the previous example, the velocity anisotropy is too pronounced for the weak-anisotropy equation (7) to hold, and the inversion does not provide an accurate value of $\varepsilon - \delta$, unless we have a good estimate of the vertical velocity.

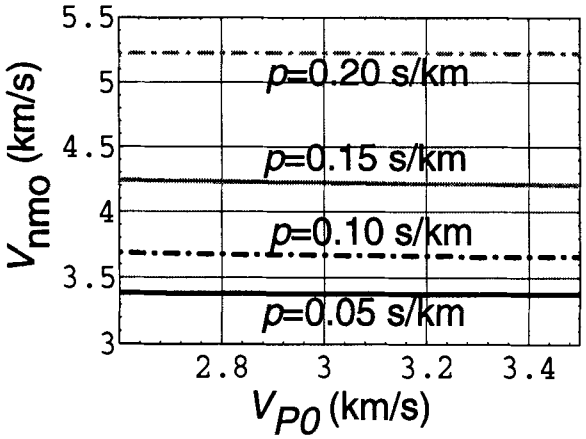

FIG. 6. NMO velocity for the family of solutions in Figure 5 and four different values of the ray parameter.

The accuracy of the estimation of $\varepsilon - \delta$ is further illustrated in Figure 8, which shows the inversion results for the models with $\varepsilon - \delta = 0.1$, 0.2, and 0.3. While the recovery of $\varepsilon - \delta$ is unique for elliptical anisotropy ($\varepsilon = \delta$, not shown on the plot), it becomes less accurate with increasing $\varepsilon - \delta$.

In essence, we have shown that the exact NMO velocity expressed through ray parameter depends just on the zero-dip NMO velocity and some combination of the anisotropy parameters close to the difference $\varepsilon - \delta$. This conclusion is in agreement not only with the weak-anisotropy equation (7), but also with the analysis of the Jacobian matrix in the previous section (it explains the ambiguity in the inversion for all three parameters—V_{P0}, ε, and δ).

Description of the equivalent solutions

Clearly, the combination of ε and δ that describes the family of ES deviates from the difference $\varepsilon - \delta$ with increasing anisotropy. An analytic description of this combination for arbitrary strength of the anisotropy is given below.

We have shown that all ES obtained by our inversion technique have the same dip-dependent NMO velocity, including that for a horizontal reflector. Therefore,

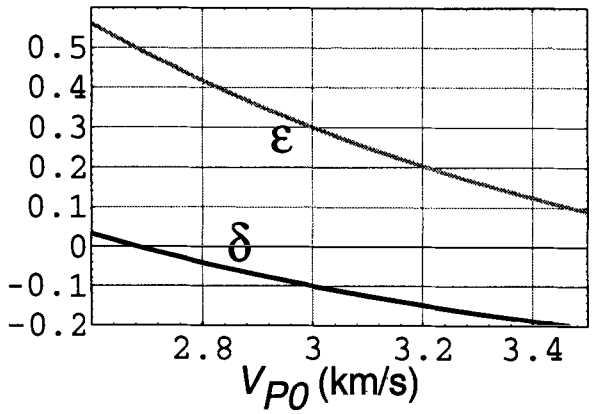

FIG. 7. Inverted values of ε and δ as functions of V_{P0} for the model with V_{P0} = 3.0 km/s, ε = 0.3, and δ = −0.1.

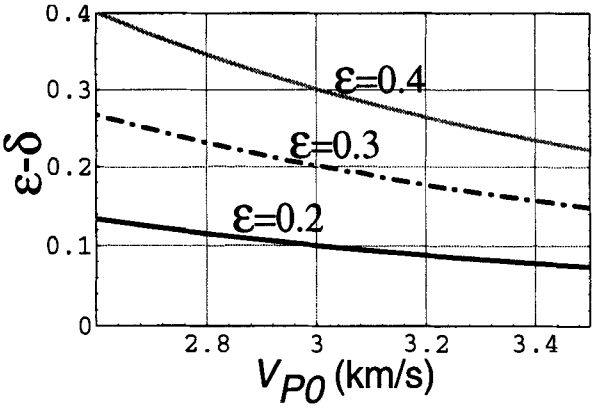

FIG. 8. Inverted value of $\varepsilon - \delta$ as a function of V_{P0} for three models with different ε; V_{P0} = 3.0 km/s, δ = 0.1.

$$V_{\rm nmo}(0) = V_{P0}\sqrt{1+2\delta} = const \qquad (9)$$

within the family of ES. This equation provides a relation between V_{P0} and δ that accurately describes the curves $\delta(V_{P0})$ in Figures 5 and 7.

However, a single equation is not sufficient to characterize the ES analytically. To obtain another relation between the parameters that would involve ε, we examine the behavior of group-velocity curves for the family of ES. Figure 9 shows the group velocity as a function of the group angle for three solutions corresponding to V_{P0} = 2.8, 3.0, and 3.2 km/s. The computations were performed for the two models shown in Figures 5 and 7. For both media, all three ES yield practically the same velocity at an angle of 90°, which coincides with the actual horizontal velocity. We have obtained the same result for all other VTI models we have studied.

This implies that for all ES

$$V_h = V_{P0}\sqrt{1+2\varepsilon} = const. \qquad (10)$$

However, it is more convenient to replace the horizontal velocity by a dimensionless parameter, common for all ES, that goes to zero for isotropic media. Combining equations (9) and (10), we choose to define a new anisotropic parameter (denoted by η) as follows:

$$\eta \equiv 0.5\left(\frac{V_h^2}{V_{\rm nmo}^2} - 1\right) = \frac{\varepsilon - \delta}{1+2\delta}. \qquad (11)$$

Then

$$V_h = V_{\rm nmo}(0)\sqrt{1+2\eta} \qquad (12)$$

[compare the form with equations (9) and (10)]. Therefore, our family of ES can be described by two effective parameters: $V_{\rm nmo}(0)$ (or V_h) and η. Only these parameters can be resolved by inverting dip-dependent P-wave NMO velocities. In principle, two distinct dips are sufficient to recover the values of $V_{\rm nmo}(0)$ and η; additional dipping reflectors just provide redundancy in the inversion procedure, so that, for example, a least-square approach can be used to solve the overdetermined problem.

Although this result for strong anisotropy has been obtained numerically, it is in good agreement with our analytic weak-anisotropy approximation (7). Essentially, by performing numerical inversion we have generalized the weak-anisotropy equation (7) to transversely isotropic media with arbitrary strength of anisotropy. While the weak-anisotropy P-wave NMO equation (expressed through ray parameter) is a function of $V_{\rm nmo}(0)$ and $\varepsilon - \delta$, the P-wave NMO velocity for general transverse isotropy is fully characterized by $V_{\rm nmo}(0)$ and η. Clearly, in the limit of weak anisotropy, η reduces to the difference $\varepsilon - \delta$. The family of ES from our first example in Figure 5 can be represented by $V_{\rm nmo}$ = 3.29 km/s and η = 0.0833. The example from Figure 7 is characterized by $V_{\rm nmo}$ = 2.68 km/s and a much larger η = 0.5.

Also, note that η is zero not only for isotropy, but also for elliptical anisotropy. In this sense, it is similar to the parameter $\sigma = (V_{P0}^2/V_{S0}^2)(\varepsilon - \delta)$ introduced in Tsvankin and Thomsen (1994) to describe SV-wave moveout.

The dominant role of the parameter η is illustrated in Figure 10a, which shows that the P-wave dip-moveout signature does not depend on the individual values of the anisotropy parameters ε and δ, if η is fixed. Both plots in Figure 10 demonstrate that for the most typical case, $\eta > 0$ ($\varepsilon > \delta$), the conventional DMO expression (6) for isotropic media severely understates NMO velocities for dipping reflectors.

While η is determined by the values of the zero-dip moveout velocity and the horizontal velocity, the choice of η is not unique. We could have combined $V_{\rm nmo}(0)$ and V_h in a different fashion to obtain, for instance, 1 + 2ε instead of 1 + 2δ in the denominator of η. However, any such anisotropic parameter describing the dip-dependence of NMO velocity would represent a measure of "nonellipticity," i.e., deviation from the elliptically anisotropic model. As we will see later, our parameter η is very convenient in characterizing nonhyperbolic moveout and other seismic signatures.

Equation (11) leads us to another observation. If it is possible to obtain an accurate value for the horizontal velocity V_h (e.g., from head waves traveling along a hori-

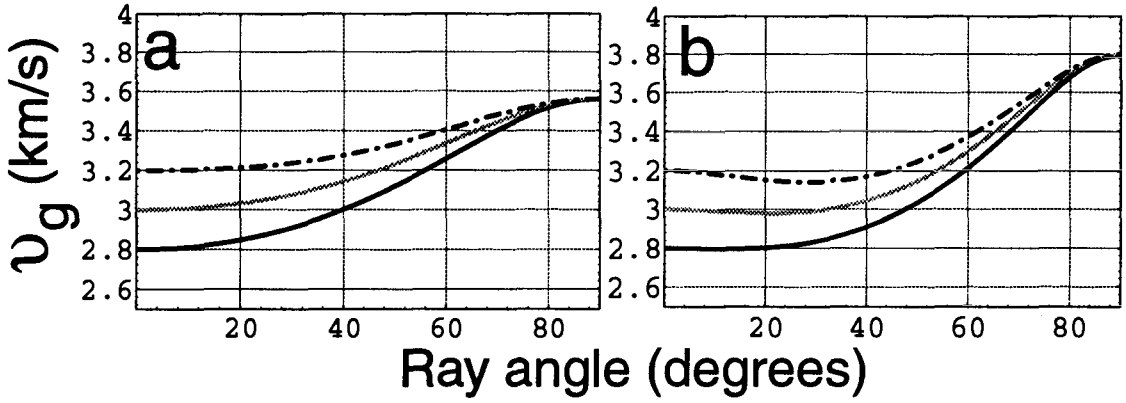

FIG. 9. Group velocity v_g as a function of the group (ray) angle for solutions from (a) Figure 5 (V_{P0} = 3.0 km/s, ε = 0.2, δ = 0.1), and (b) Figure 7 (V_{P0} = 3.0 km/s, ε = 0.3, δ = −0.1). The curves correspond to solutions with V_{P0} = 2.8 km/s and the corresponding values of δ and ε (black); V_{P0} = 3.0 km/s (actual values, gray); and V_{P0} = 3.2 km/s (dashed).

zontal reflector or from crosswell tomography), then the zero-dip velocity $V_{nmo}(0)$ is sufficient to find η and to build the P-wave NMO velocity as a function of ray parameter. Dipping reflectors in this case are not needed at all.

As demonstrated in the following sections, the importance of the family of ES goes well beyond the dip-dependence of P-wave NMO velocities.

Accuracy of the inversion

Next, we study the sensitivity of the inversion procedure to errors in the measured moveout velocities. In the typical case of a horizontal and dipping reflector, we measure two velocities: $V_{nmo}(p)$ and $V_{nmo}(0)$. Since $V_{nmo}(0)$ is obtained directly, η remains the only unknown to be solved for. As illustrated by Figure 10b, the NMO-velocity curves corresponding to $\eta = 0.1$, 0.2, and 0.3 are well resolved within a wide range of dips, which indicates that the inversion procedure is reasonably stable.

To quantify errors in η, we use the following sensitivity equation:

$$\Delta V_{nmo}(p) = \frac{\partial V_{nmo}(p)}{\partial V_{nmo}(0)} \Delta V_{nmo}(0) + \frac{\partial V_{nmo}(p)}{\partial \eta} \Delta\eta. \quad (13)$$

Normalizing the velocities, we can represent equation (13) as

$$\frac{\Delta V_{nmo}(p)}{V_{nmo}(p)} = \frac{V_{nmo}(0)}{V_{nmo}(p)} \frac{\partial V_{nmo}(p)}{\partial V_{nmo}(0)} \frac{\Delta V_{nmo}(0)}{V_{nmo}(0)} + \frac{1}{V_{nmo}(p)} \frac{\partial V_{nmo}(p)}{\partial \eta} \Delta\eta. \quad (14)$$

Using equation (14), the error in η can be expressed through the errors in the NMO velocities,

$$\Delta\eta = \left[\frac{V_{nmo}(p)}{f_2}\right] \frac{\Delta V_{nmo}(p)}{V_{nmo}(p)} - \left[f_1 \frac{V_{nmo}(0)}{f_2}\right] \frac{\Delta V_{nmo}(0)}{V_{nmo}(0)}, \quad (15)$$

where

$$f_1 = \frac{\partial V_{nmo}(p)}{\partial V_{nmo}(0)}$$

and

$$f_2 = \frac{\partial V_{nmo}(p)}{\partial \eta}.$$

If the NMO velocity for a horizontal reflector is measured exactly or contains only a small error, the error in η would be controlled just by the first term in formula (15). However, assuming that the errors in $V_{nmo}(p)$ and $V_{nmo}(0)$ have comparable magnitude, we can characterize the sensitivity of η by

$$E = \frac{\sqrt{V_{nmo}^2(p) + [f_1 V_{nmo}(0)]^2}}{f_2}. \quad (16)$$

Figure 11 shows E as a function of the ray parameter for the models from Figures 5 and 7. In both examples, as expected, errors decrease with dip and reach a minimum at a dip of about 46° (a), and 51° (b). The minimum in E is caused by higher sensitivity to errors in $V_{nmo}(0)$ at steep dips; if the error in $V_{nmo}(0)$ is negligibly small, the minimum does not exist, and the inversion for η is most stable at steep dips up to 90°.

However, in the discussion above we have not considered two factors that make steep dips (beyond 50–60°) less desirable in the inversion algorithm. First, at steep dips the inversion for η becomes more sensitive to errors in the ray parameter [see Figure 10b]. Second, the recovery of the NMO velocity itself from reflection moveouts becomes less stable because the magnitude of the quadratic moveout term decreases with dip (because of higher NMO velocity).

It may be also instructive to examine numerically the sensitivity of the effective parameter η and the horizontal velocity V_h [equation (12)] to errors in the measured values of $V_{nmo}(p)$. In Figure 12, we have introduced errors into the input values of NMO velocities for reflector dips of 0 and 40°. The percentage error in V_h and the absolute error in η

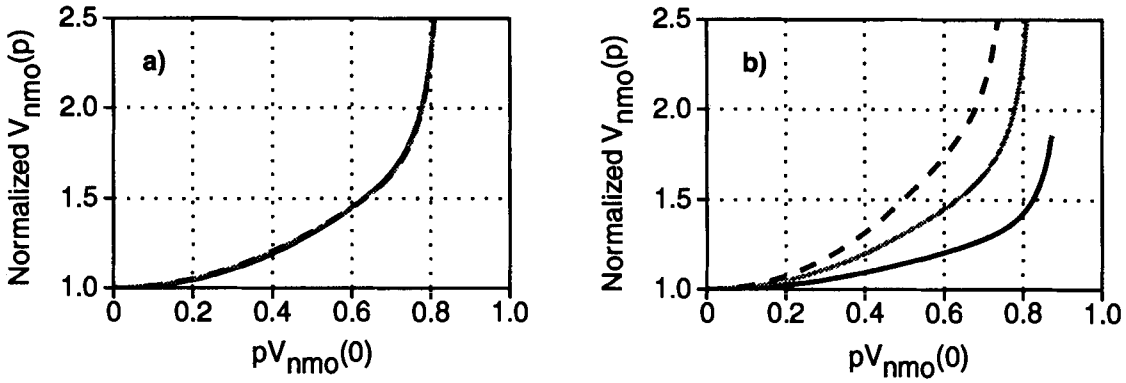

FIG. 10. P-wave moveout velocity calculated from formula (1) and normalized by the expression for isotropic media (6). The dip angles range between 0 and 70°. (a) Different models with the same $\eta = 0.2$: $\varepsilon = 0.1$, $\delta = -0.071$ (solid black); $\varepsilon = 0.2$, $\delta = 0$. (gray); $\varepsilon = 0.3$, $\delta = 0.071$ (dashed)—the curves practically coincide with each other. (b) Models with different η: $\eta = 0.1$ (solid black); $\eta = 0.2$ (gray); $\eta = 0.3$ (dashed).

are quite small, which indicates that our inversion is reasonably stable. In fact, a 5% error in $V_{\text{nmo}}(p)$ causes less than a 2.5% error in V_h. The percentage error in η is larger, but this can be expected in the inversion for so small an anisotropic coefficient.

PROPERTIES OF THE FAMILY OF SOLUTIONS

Nonhyperbolic reflection moveout

The inversion of the dip-dependence of P-wave normal moveout velocities enables one to obtain a family of equivalent solutions (ES) described by the zero-dip NMO velocity $V_{\text{nmo}}(0)$ and the effective anisotropic parameter η. In this section, we show a remarkable property of ES: any model with the same $V_{\text{nmo}}(0)$ and η yields the same long-spread (nonhyperbolic) P-wave moveout from a horizontal reflector.

P-wave long-spread moveout in horizontally layered transversely isotropic media can be well-approximated by the following equation (Tsvankin and Thomsen, 1994):

$$t^2(X) = t_{P0}^2 + A_2 X^2 + \frac{A_4 X^4}{1 + AX^2}, \tag{17}$$

where t_{P0} is the two-way, zero-offset time.

For a single layer, the coefficients in formula (17) are

$$A_2 = \frac{1}{V_{P0}^2(1 + 2\delta)} = \frac{1}{V_{\text{nmo}}^2(0)},$$

$$A_4 = -\frac{2(\varepsilon - \delta)}{t_{P0}^2 V_{P0}^4} \frac{1 + \dfrac{2\delta}{1 - V_{S0}^2/V_{P0}^2}}{(1 + 2\delta)^4},$$

and

$$A = \frac{A_4}{\dfrac{1}{V_h^2} - A_2},$$

where V_h is the horizontal velocity.

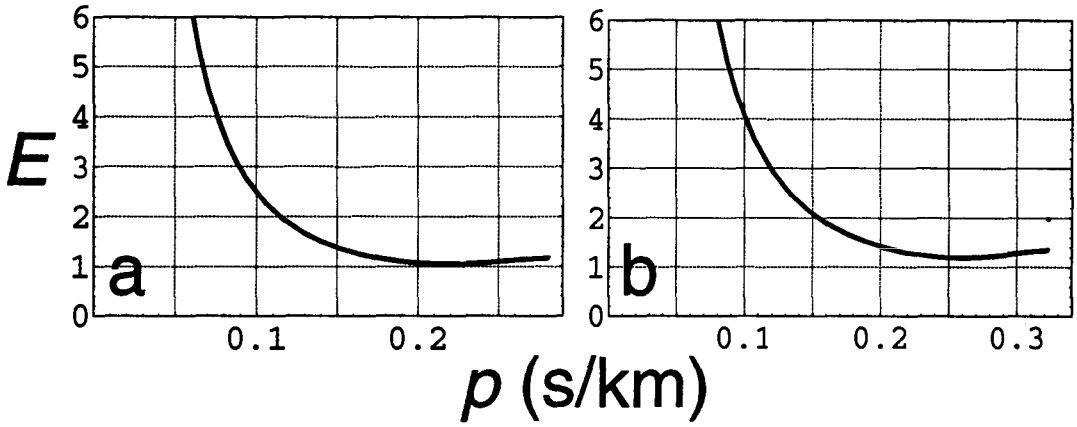

FIG. 11. E as a function of the ray parameter corresponding to the dipping reflector for (a) the model used to generate Figure 5 (V_{P0} = 3.0 km/s, ε = 0.2, δ = 0.1), and (b) the model used to generate Figure 7 (V_{P0} = 3.0 km/s, ε = 0.3, δ = −0.1).

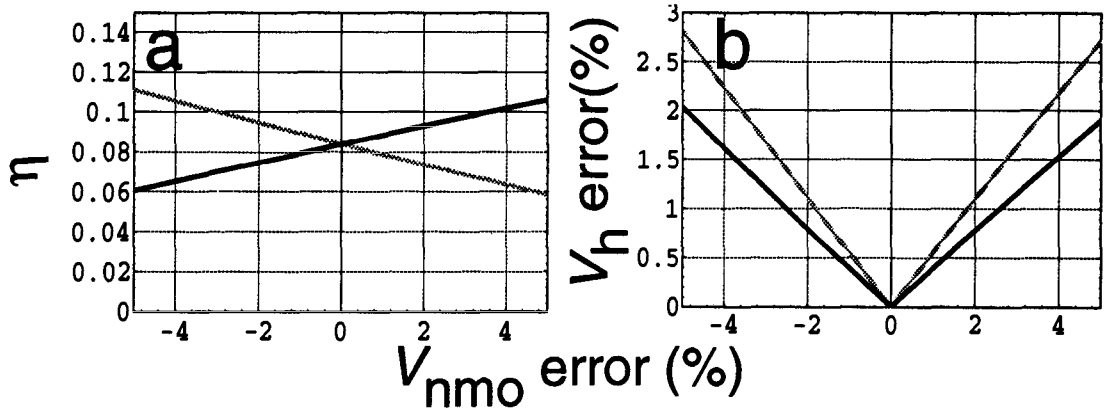

FIG. 12. Dependence of the inverted values of η (a) and V_h (b) on the error in the measured NMO velocities. The model parameters are V_{P0} = 3.0 km/s, ε = 0.2, and δ = 0.1; reflector dips of 0 and 40° were used. Black lines correspond to errors in the NMO velocity for the dipping reflector only. Gray lines correspond to identical errors in both V_{nmo} values.

Equation (17) remains numerically accurate for long spreads (two to three times, and more, the reflector depth) and pronounced anisotropy. The hyperbolic moveout term, which makes the main contribution to short-spread moveout, depends on just the NMO velocity $V_{\text{nmo}}(0)$. The last term in equation (17) describes nonhyperbolic moveout on long spreads.

Substituting the parameters $V_{\text{nmo}}(0)$ and η into formula (17) and ignoring the contribution of V_{S0} to the quartic term A_4 (V_{S0} has a negligible influence on P-wave moveout in TI media), we obtain

$$t^2(X) = t_{P0}^2 + \frac{X^2}{V_{\text{nmo}}^2(0)} - \frac{2\eta X^4}{V_{\text{nmo}}^2(0)[t_{P0}^2 V_{\text{nmo}}^2(0) + (1 + 2\eta)X^2]}. \quad (18)$$

Thus, P-wave long-spread moveout can be adequately described by just the vertical traveltime and the two effective parameters, $V_{\text{nmo}}(0)$ and η, with no separate dependence on V_{P0}, ε, or δ. For given $V_{\text{nmo}}(0)$ and t_{P0}, η describes the amount of deviation from hyperbolic moveout; if $\eta = 0$, the medium is elliptical and the moveout is purely hyperbolic.

Although equation (17) is approximate, and we have made one more small approximation by assuming that $V_{S0} = 0$, the results in the next section prove that P-wave long-spread moveout is indeed controlled by $V_{\text{nmo}}(0)$ and η. Since the inversion algorithm makes it possible to recover $V_{\text{nmo}}(0)$ and η, it provides enough information to build P-wave long-spread moveout curves. Stated differently, although the inversion is unable to resolve V_{P0}, ε, and δ, the two parameters it gives are sufficient to describe P-wave long-spread moveout.

Migration impulse response

Although equation (18) describes moveout for a horizontal reflector, it also can be regarded as the diffraction curve, accurate to a certain dip, on the zero-offset section (poststack domain). Since time migration is based on collapsing such diffraction curves to their apexes, the values of $V_{\text{nmo}}(0)$ and η should be sufficient to generate a time-migration impulse response that is accurate up to that certain dip. With accurate values of $V_{\text{nmo}}(0)$ and η, all lateral position errors in migration for homogeneous models (Larner and Cohen, 1993; Alkhalifah and Larner, 1994) will be eliminated. Poststack depth migration, however, may produce depth errors if the value of V_{P0} is inaccurate, but this is a different issue.

Figure 13 shows the exact time-migration impulse responses (right half only) for different ES from (a) Figure 5 and (b) Figure 7. The curves for all three ES practically coincide with each other, implying that there is no difference between the impulses of the three input models. This confirms that $V_{\text{nmo}}(0)$ and η are sufficient to generate an accurate time-migration impulse response for all dips.

This point is illustrated further by Figure 15, which shows anisotropic poststack time migrations [Gazdag's (1978) phase-shift migration modified for anisotropic media (Kitchenside, 1991)] of the synthetic data generated for the model in Figure 14. The reflectors are embedded in a homogeneous transversely isotropic medium with $V_{P0} = 3.0$ km/s, $\varepsilon = 0.2$, and $\delta = 0.1$ (the same model as in Figure 5, $V_{\text{nmo}}(0) = 3.29$ km/s, $\eta = 0.0833$). The migrations were performed (a) using the actual model parameters, and (b) using an equivalent solution from Figure 5 with $V_{P0} = 2.6$ km/s, $\varepsilon = 0.433$, and $\delta = 0.3$. Although model (b) is substantially different from the actual one, it has the correct values of $V_{\text{nmo}}(0)$ and η and, consequently, produces an accurate image (the artifact below the steep reflector is caused by the limited aperture).

Depth migration, however, will produce depth errors if the wrong value of V_{P0} were used. Such depth errors ΔD can be described by

$$\Delta D = \left(\frac{V_{P0}}{V_{\text{actual}}} - 1\right) D,$$

where V_{actual} is the true vertical velocity, and D is the true depth.

Therefore, all ES have the same poststack depth migration impulse response with a simple depth stretch. As we show in the next section, errors in the effective parameters $V_{\text{nmo}}(0)$ and η lead to distortions in migrated images.

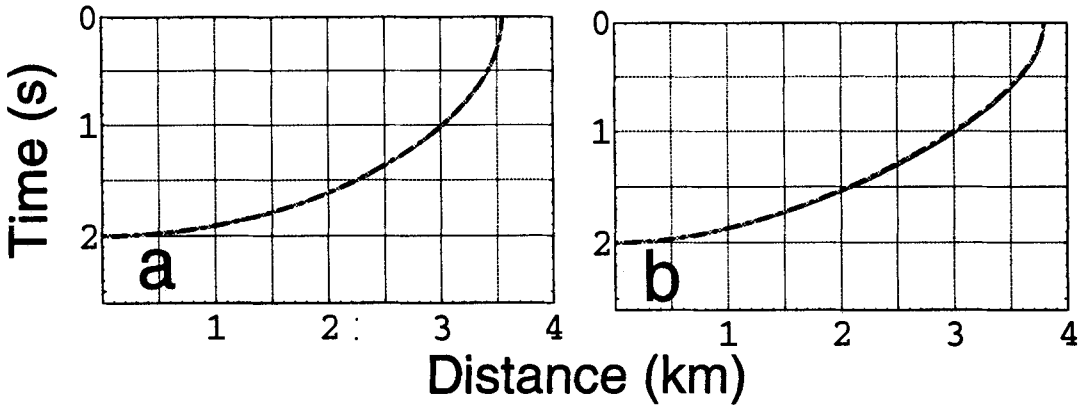

FIG. 13. Anisotropic time-migration impulse response for solutions from (a) Figure 5, and (b) Figure 7. The three curves on each plot correspond to the solutions with $V_{P0} = 2.8$ km/s (solid black), 3 km/s (gray), and 3.2 km/s (dashed). All three curves practically coincide with each other.

Since all ES characterized by $V_{nmo}(0)$ and η have the same NMO velocity $V_{nmo}(p)$ in the prestack domain and the same time-migration impulse response in the poststack domain, they should also have the same time-migration impulse in the prestack domain. Thus, media with the same $V_{nmo}(0)$ and η yield the same prestack and poststack diffraction curves for surface seismic data.

We conclude that the inversion of P-wave NMO velocities provides enough information to perform all major time-processing steps including dip moveout (DMO), and prestack and poststack time migration. However, time-to-depth conversion requires an accurate value of the vertical velocity, which cannot be obtained from NMO velocities alone.

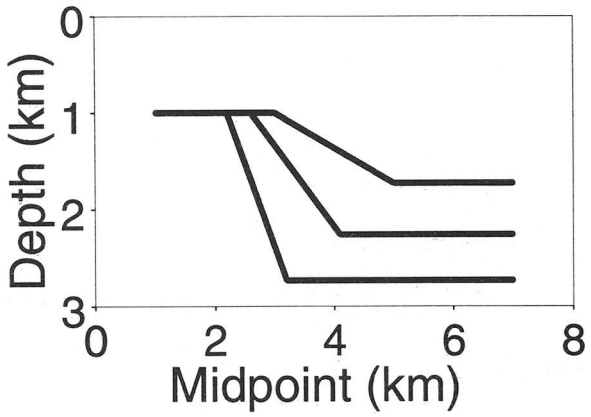

FIG. 14. Model with reflectors dipping at 0, 20, 40, and 60 degrees.

REFINING INVERSION RESULTS USING POSTSTACK MIGRATION

In many cases, one can determine the accuracy of the migration algorithm or of the velocity field used in the migration by observing the quality of the migrated image. For example, parabolic shapes, resulting from diffracting edges, imply overmigration, whereas hyperbolic shapes indicate undermigration.

This approach can be used to refine the results of our inversion procedure. Errors in the measured NMO velocity may lead to an inaccurate value of η, which in turn, may distort the migrated image. Figure 16 shows anisotropic poststack time migration of a synthetic data set generated for the model in Figure 14 using inaccurate values of η (the correct value, V_{nmo} = 3.29 km/s, is used in both cases). The errors, apparent in both cases, show the sensitivity of the migration results to the value of η. Predictably, the distortions are more pronounced for the model with a larger error in η: not only do the reflectors cross, but also the reflector edges are not imaged well. The dipping events can be imaged better by increasing the value of $V_{nmo}(0)$, but in this case the horizontal reflectors go out of focus.

Usually we can expect to obtain the zero-dip NMO velocity with a higher accuracy than that for the parameter η. The inverted value of η, however, can be refined by inspecting migrated images. In isotropic media, undermigration is usually corrected by increasing the migration velocity. According to equation (12), an increase in η leads to a

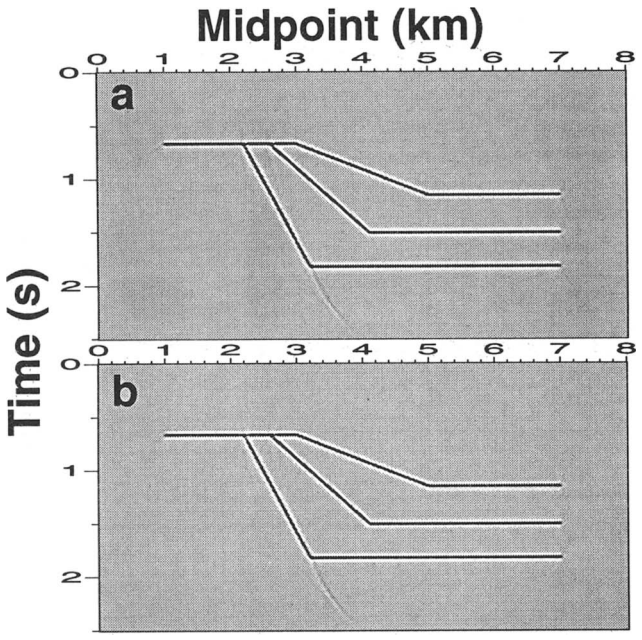

FIG. 15. Anisotropic time migrations of synthetic data generated for the model in Figure 14 ($V_{nmo}(0)$ = 3.29 km/s, η = 0.0833) using (a) the actual model values of V_{P0} = 3.0 km/s, ε = 0.2, and δ = 0.1; and (b) an equivalent solution V_{P0} = 2.6 km/s, ε = 0.433, and δ = 0.3.

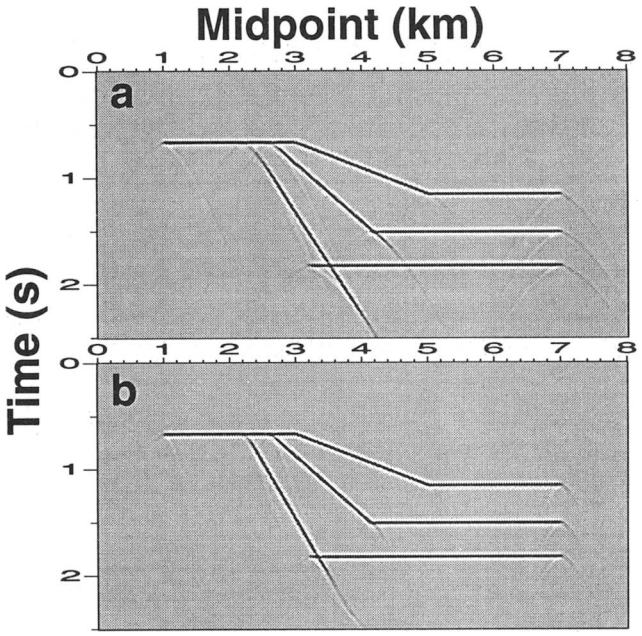

FIG. 16. Anisotropic poststack time migrations of a synthetic data set generated for the model in Figure 14 using distorted values of η: (a) η = 0.01, (b) η = 0.06; the actual value η = 0.0833. In both cases $V_{nmo}(0)$ = 3.29 km/s, the correct value.

higher horizontal velocity. Therefore, a corresponding correction in transversely isotropic media can be achieved by increasing η (the case in Figure 16, where too small values of η cause undermigration).

However, if we have more confidence in the measured value of the NMO velocity for the dipping reflector, a proper choice would be to change both $V_{\mathrm{nmo}}(0)$ and η. In fact, given that error likely exists in both, the data processor now has two parameters that can be adjusted.

VELOCITY ANALYSIS IN A LAYERED MEDIUM

The inversion technique discussed above is designed for a homogeneous medium above the reflector, while realistic subsurface models are, at a minimum, vertically inhomogeneous. In Appendix B we extend the NMO equation given by Tsvankin (1995) to layered anisotropic media; here we show that this new equation can be used to recover the NMO velocity in the medium immediately above the reflector via a Dix-type formula.

We assume that the model consists of a stack of plane homogeneous layers above a dipping reflector. The incidence plane should coincide with the dip plane of the reflector and a plane of symmetry in all layers (although the symmetries themselves may be different). If a layer is transversely isotropic, the incidence plane should contain the symmetry axis (or it may be the isotropy plane); in an orthorhombic medium, the incidence plane should coincide with one of the three mutually orthogonal symmetry planes.

As shown in Appendix B, the normal-moveout velocity for such a model is given by

$$V^2_{\mathrm{nmo}}(p_0) = \frac{1}{t_0} \sum_{i=1}^{n} t_0^{(i)} [V^{(i)}_{\mathrm{nmo}}(p_0)]^2. \qquad (19)$$

That is, the NMO velocity is the root-mean-square of the NMO velocities in each layer given by equation (1) and taken at the ray-parameter value p_0 determined by the dipping reflector: $p_0 = \sin\phi/V^{(n)}(\phi)$, where ϕ is the dip angle, and $V^{(n)}$ is the phase velocity immediately above the dipping reflector. The traveltimes $t_0^{(i)}$ should be calculated along the zero-offset ray. Equation (19) is quite general in the sense that it does not assume any specific type of anisotropy, although it does require the incidence plane to be a plane of symmetry. For isotropic media, formula (19) becomes equivalent to the NMO expression in Shah (1973).

If the reflector is horizontal, equation (19) reduces to the root-mean-square (rms) of the zero-dip NMO velocities; however, unless the medium is transversely isotropic with a vertical symmetry axis (VTI), the zero-offset ray may deviate from the vertical direction, and t_0 may be different from the vertical time. For the special case of a stack of horizontal VTI layers, formula (19) coincides with the well-known expression discussed in Hake et al. (1984) and Tsvankin and Thomsen (1994).

To obtain the NMO velocity in any layer i (including the one immediately above the reflector), we need to apply the Dix formula (Dix, 1955) to the NMO velocities from the top $[V_{\mathrm{nmo}}(i-1)]$ and bottom $[V_{\mathrm{nmo}}(i)]$ of the layer:

$$[V^{(i)}_{\mathrm{nmo}}]^2 = \frac{t_0(i)V^2_{\mathrm{nmo}}(i) - t_0(i-1)V^2_{\mathrm{nmo}}(i-1)}{t_0(i) - t_0(i-1)}, \qquad (20)$$

where $t_0(i-1)$ and $t_0(i)$ are the two-way traveltimes to the top and bottom of the layer, respectively, calculated along the ray with $p = p_0$. All NMO velocities here correspond to the ray-parameter value p_0.

The main difference between the NMO equation (20) and the conventional Dix formula is that all NMO velocities and traveltimes in formula (20) should be evaluated at the ray-parameter value corresponding to the dip angle of the reflector $[p_0 = \sin\phi/V^{(n)}(\phi)]$. Suppose, we are interested in using equation (20) to obtain the normal moveout velocity in the medium immediately above the reflector $[V^{(n)}_{\mathrm{nmo}}(p_0)]$ that can serve as an input value in the inversion algorithm discussed in the previous sections. Clearly, the recovery of $V^{(n)}_{\mathrm{nmo}}(p_0)$ is impossible without obtaining the moveout velocities in the overlying medium for the same value of the ray parameter, p_0. This task is not trivial because conventional NMO velocity analysis for the horizontally layered overburden provides us only with NMO velocities and traveltimes corresponding to the ray-parameter value $p = 0$.

However, for the special case of isotropic or elliptically anisotropic horizontal layers, the normal moveout velocity at any ray-parameter value can be obtained from the zero-dip NMO velocity in a straightforward fashion [equation (6)]. To apply equations (19) and (20), it is also necessary to express the traveltime $t_0(p)$ through the zero-offset time $t_0(0)$ and NMO velocity for a horizontal reflector. In Appendix B, we derive an equation for $t_0(p)$ valid for isotropy or elliptical anisotropy:

$$t_0(p) = t_0(0)\sqrt{1 + p^2V^2_{\mathrm{nmo}}(p)}. \qquad (21)$$

Therefore, if the overburden layers are isotropic or elliptically anisotropic, the two-way traveltime along the ray with any ray-parameter value p can be found just from the vertical traveltime $t_0(0)$ and the NMO velocity $V_{\mathrm{nmo}}(p)$ already determined from equation (6).

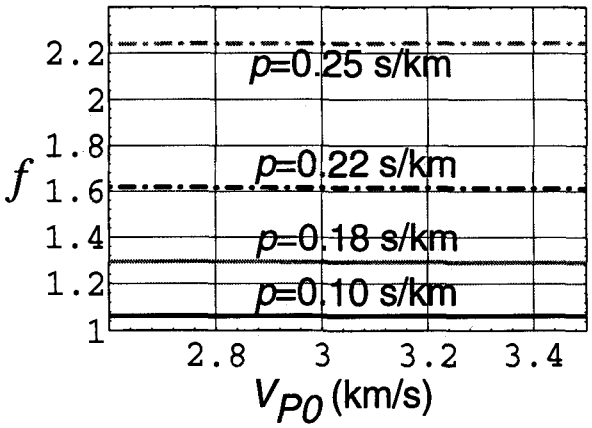

FIG. 17. Curves of the value of $f = t_0(p)/t_0(0)$ in equation (22), for a range of equivalent solutions and four different values of the ray parameter p. Here, $V_{nmo} = 3.29$ km/s and $\eta = 0.0833$.

If the horizontal layers are vertically transversely isotropic (but not elliptically anisotropic), we have seen that it is necessary to know the value of η in addition to the zero-dip NMO velocity to find $V_{\rm nmo}(p)$. As illustrated in Figure 17, the parameters $V_{\rm nmo}(0)$ and η are also sufficient to calculate $t_0(p)$ given the zero-dip time $t_0(0)$:

$$t_0(p) = t_0(0) f[\eta, V_{\rm nmo}(0)], \qquad (22)$$

where f is independent of the vertical velocity and the individual values of the anisotropies ε and δ.

Thus, we propose the following processing sequence designed to strip the influence of the overburden on the NMO velocity: obtain the zero-dip NMO velocities and zero-offset traveltimes for the horizontal layers, use these values to calculate the NMO velocity and traveltime at the ray-parameter value p_0 for the entire horizontally stratified overburden, and finally, calculate the NMO velocity for the medium immediately above the dipping reflector via the Dix-type formula (20). In the case when the overburden is not elliptically anisotropic, this stripping algorithm requires η in the overburden to be estimated independently. If only surface P-wave data are available, the recovery of η requires the presence of dipping reflectors in all layers.

The normal moveout velocity obtained for the layer immediately above the dipping reflector (corresponding to the ray-parameter value p_0) should be combined with the NMO velocity measured for some other dip $p \neq p_0$ (e.g., the zero-dip NMO velocity) for the same layer to perform the single-layer inversion procedure discussed in the previous sections.

The nonhyperbolic moveout equation for a horizontally layered, transversely isotropic medium (17) is a function of the quadratic (A_2) and quartic (A_4) moveout coefficients and horizontal velocities (V_h) in each layer, averaged in a complicated fashion (Tsvankin and Thomsen, 1994). Since A_2, A_4, and V_h in individual layers depend just on $V_{\rm nmo}(0)$ and η, the total moveout curve is entirely determined by the values of these two effective parameters averaged over the stack of layers. Likewise, this conclusion holds for time migration in $V(z)$ media.

FIELD-DATA EXAMPLE

Figure 18 shows a seismic line from offshore Africa provided to us by Chevron Overseas Petroleum, Inc. The line was processed using a sequence of conventional NMO, DMO, and time-migration algorithms without taking anisotropy into account. While horizontal and mildly dipping reflectors are imaged well, steeply dipping fault planes (like the one at a time of 1.5–2 s to the left of CMP 1000) are almost invisible.

To demonstrate that this problem is caused by anisotropy, it is useful to examine constant-velocity CMP stacks (stacks generated at certain constant values of the stacking velocity) after application of normal-moveout correction followed by conventional constant-velocity DMO (Figure 19). The goal of DMO processing is to focus both horizontal and dipping events on the same velocity panel. However, while subhorizontal reflectors are imaged best at a stacking velocity of 2200 m/s, the dipping reflector goes into focus at a much higher velocity (2400–2450 m/s). As a result, the conventional processing sequence produces a weak, blurry image of the dipping fault plane.

The failure of conventional DMO means that the stacking (moveout) velocity increases with dip much faster than implied by the isotropic equation (6) (Figure 10). If the DMO problem had been caused by velocity gradient, than the dipping event would have been imaged at a *lower* stacking velocity than that of the horizontal event (Hale and Artley, 1993). Therefore, the DMO algorithm breaks down as a result of the increase in the stacking velocity for dipping reflectors caused by anisotropy.

We have picked the best-fit stacking velocities and the corresponding ray parameters for the subhorizontal and dipping events from constant-velocity stacks and applied our inversion algorithm for a homogeneous VTI medium. The inversion procedure yielded the value of $\eta = 0.07$, which was used to reprocess the data by means of a TZO (transformation to zero offset) ray-tracing algorithm designed for homogeneous VTI models (Alkhalifah, 1994). The anisotropic TZO succeeded in focusing both the subhorizontal and dipping events on the same velocity panel—the one corresponding to the best-fit stacking velocity for the subhorizontal reflector (Figure 20).

The anisotropic processing sequence described above was based on the assumption that the medium above the dipping reflector is homogeneous. However, analysis of time dependence of the zero-dip stacking (moveout) velocity [which can be approximated by $V_{\rm nmo}(0)$] shows a pronounced velocity gradient of about 0.7 s^{-1}. Therefore, the value of η produced by the inversion algorithm can be regarded as an effective parameter that reflects the influence of both anisotropy and inhomogeneity (Tsvankin, 1995). While this effective η enabled us to correct for the influence of anisotropy in DMO processing (because we had just a single dipping event), it cannot be used in anisotropic poststack migration or inversion for the individual values of ε and δ.

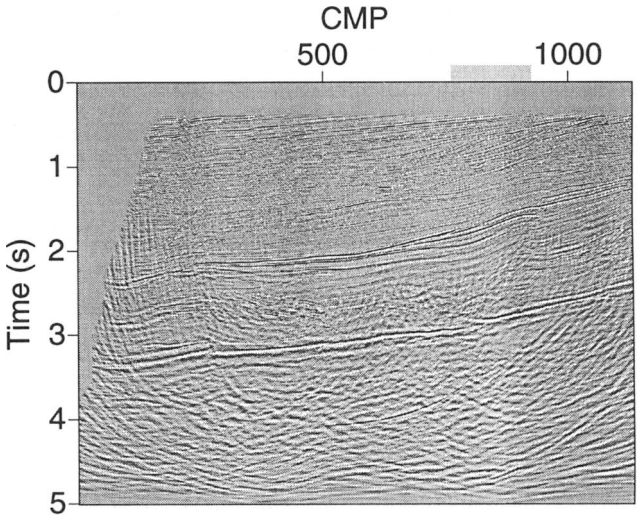

FIG. 18. Time-migrated seismic line (offshore Africa). The gray bar to the left of CMP 1000 shows the CMP gathers that we will examine in Figures 19 and 20.

This example represents no more than a preliminary result that illustrates the importance of anisotropic data processing and some practical aspects of the application of our algorithm. More robust processing results in the presence of velocity gradient may be achieved by using the NMO equation for a vertically inhomogeneous medium [formula (19)]; this will be discussed in detail in a sequel paper.

DISCUSSION AND CONCLUSIONS

We have suggested and tested, on synthetic and real data, a method of velocity analysis for transversely isotropic media based on the inversion of the dip-dependence of *P*-wave normal moveout velocities. The algorithm, operating with surface *P*-wave data only, requires NMO velocities and ray parameters to be measured for two different dips; more than two dips provide redundancy that can be used to increase the accuracy of the inversion.

Although this inversion cannot resolve the vertical velocity and anisotropic coefficients individually, it makes it possible to obtain a family of models that have the same moveout velocity for a horizontal reflector $V_{nmo}(0)$ and the same effective anisotropic parameter $\eta = (\varepsilon - \delta)/(1 + 2\delta)$. We have shown that these two parameters are sufficient to obtain NMO velocity as a function of ray parameter, to describe long-spread (nonhyperbolic) reflection moveout for a horizontal reflector, and to calculate poststack and prestack time-migration impulse responses. (The influence of the shear-wave vertical velocity on *P*-wave moveout is small.) This means that the inversion of *P*-wave NMO velocities provides enough information to perform all major time-processing steps, including dip moveout and prestack and poststack time migration.

The results of the inversion for η can be refined by inspecting the quality of images generated by poststack migration algorithms. If the image indicates undermigration, we should increase the value of η; to correct for overmigration, η needs to be reduced.

A natural way to include this inversion technique in the processing flow is to apply a Fowler-type dip-moveout method (Fowler, 1984), which transforms CMP data into constant-velocity stacks calculated for a range of stacking velocities. These constant-velocity panels can be conveniently used to pick NMO velocities as well as the corresponding ray parameters required for the inversion procedure. The values of $V_{nmo}(0)$ and η can then be refined by inspecting the output stacked panels generated by resampling in the frequency-wavenumber ($\omega - k$) domain using anisotropic NMO equation (1). These ideas are discussed in more detail in Anderson et al. (1994).

Our analysis suggests an alternative approach to the inverse problem. If it is possible to obtain an accurate value for the horizontal velocity V_h (e.g., from head waves traveling along a horizontal reflector or from crosshole tomography), then the zero-dip velocity $V_{nmo}(0)$ is sufficient to find η and, therefore, to perform the processing steps mentioned above. Dipping reflectors in this case are not needed at all.

Time-to-depth conversion, however, requires an accurate value of the vertical velocity that cannot be found from *P*-wave NMO velocities alone. Additional information can be obtained from the short-spread moveout velocities of *SV-SV* or *P-SV* waves, which provide one more relation between the vertical velocities and the anisotropy parameters ε and δ (Tsvankin and Thomsen, 1994). Also, the vertical velocity can be determined directly if check shots or well logs are available.

The inversion algorithm described here is developed for a homogeneous, transversely isotropic medium above the reflector. To extend the method to vertically inhomogeneous media, we generalized the NMO equation given in Tsvankin

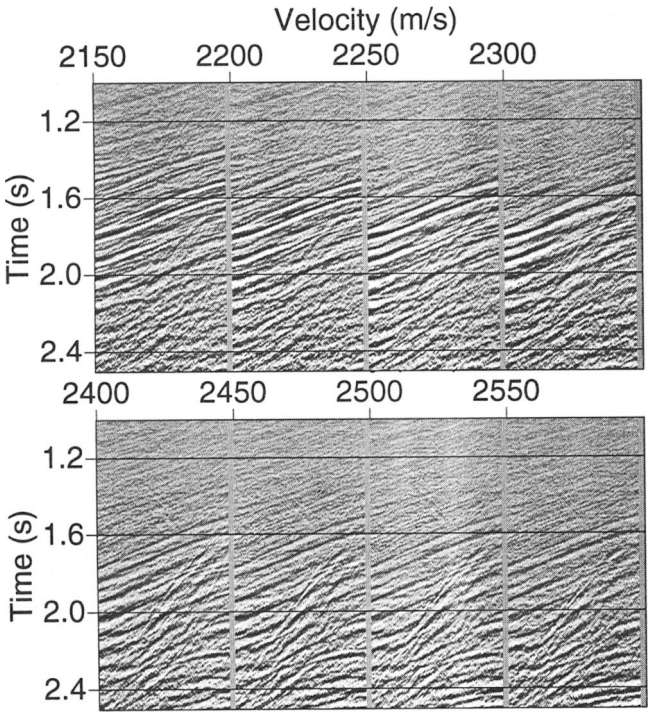

FIG. 19. Constant-velocity stacks for the area below the gray bar in Figure 18 after the conventional sequence of NMO and constant-velocity DMO (without accounting for anisotropy). The velocity values at the top correspond to the stacking velocity for horizontal reflectors.

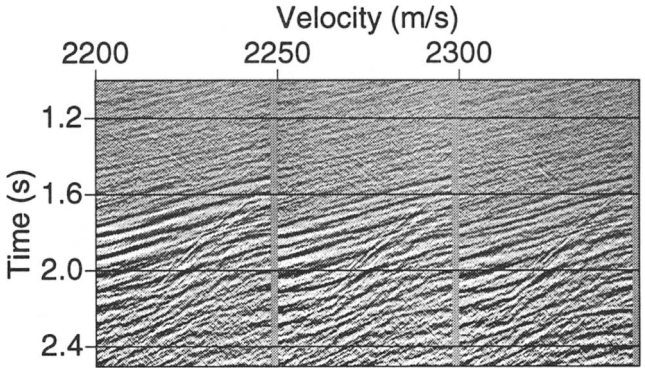

FIG. 20. Constant-velocity stacks after transformation to zero offset (TZO) adapted for homogeneous VTI media. The velocity values at the top correspond to the stacking velocity for horizontal reflectors; $\eta = 0.07$.

(1995) for layered anisotropic media with a dipping reflector. We show that the influence of a stratified isotropic or anisotropic overburden on moveout velocity can be stripped through a Dix-type differentiation procedure. This NMO formula is valid in symmetry planes of any vertically inhomogeneous anisotropic medium and, therefore, can be used in developing inversion algorithms for more complicated anisotropic models than those considered in this paper.

ACKNOWLEDGMENTS

We are grateful to Ken Larner for helpful discussions at the critical stages of this study and his review of the manuscript. We wish to thank John Toldi and Chris Dale of Chevron Overseas Petroleum, Inc. for providing the field data. Thorough reviews by Mark Meadows and Bob Hardage helped to improve the manuscript. The support for this work was provided by the members of the Consortium Project on Seismic Inverse Methods for Complex Structures at the Center for Wave Phenomena, Colorado School of Mines, and by the United States Department of Energy, Grant Number DE-FG02-89ER14079 (this support does not constitute an endorsement by DOE of the views expressed in this paper). T. Alkhalifah wishes to acknowledge the financial support from KACST (Saudi Arabia).

REFERENCES

Alkhalifah, T., 1994, Transformation to zero offset in transversely isotropic media: Center for Wave Phenomena, Colorado School of Mines (CWP-162).

——— 1995, Gaussian beam migration in anisotropic media: Geophysics, **60**, 1474–1484.

Alkhalifah, T., and Larner, K., 1994, Migration error in transversely isotropic media: Geophysics, **59**, 1405–1418.

Anderson, J., Alkhalifah, T., and Tsvankin, I., 1994, Fowler DMO and time migration for transversely isotropic media: SEG Ann. Internat. Mtg., Soc. Expl. Geophys. Expanded Abstracts, 1217–1220.

Byun, B. S., and Corrigan, D., 1990, Seismic traveltime inversion for transverse isotropy: Geophysics, **55**, 192–200.

Dix, C. H., 1955, Seismic velocities from surface measurements: Geophysics, **20**, 68–86.

Fowler, P., 1984, Velocity-independent imaging of seismic reflectors: 54th Ann. Internat. Mtg., Soc. Expl. Geophys. Expanded Abstracts, 383–385.

Gazdag, J., 1978, Wave equation migration with the phase-shift method: Geophysics, **43**, 1342–1351.

Hake, H., Helbig, K., and Mesdag, C. S., 1984, Three-term Taylor series for $t^2 - x^2$ curves over layered transversely isotropic ground: Geophys. Prosp., **32**, 828–850.

Hale, D., and Artley, C., 1993, Squeezing dip moveout for depth-variable velocity: Geophysics, **58**, 257–264.

Hale, D., Hill, N. R., and Stefani, J., 1992, Imaging salt with turning seismic waves: Geophysics, **57**, 1453–1462.

Kitchenside, P. W., 1991, Phase shift-based migration for transverse isotropy: Ann. Internat. Mtg., Soc. Expl. Geophys., Expanded Abstracts, 993–996.

Larner, K., 1993, Dip-moveout error in transversely isotropic media with linear velocity variation in depth: Geophysics, **58**, 1442–1453.

Larner, K., and Cohen, J., 1993, Migration error in transversely isotropic media with linear velocity variation in depth: Geophysics, **58**, 1454–1467.

Sena, A. G., 1991, Seismic traveltime equations for azimuthally anisotropic and isotropic media: Estimation of internal elastic properties: Geophysics, **56**, 2090–2101.

Sena, A. G., and Toksöz, M. N., 1993, Kirchhoff migration and velocity analysis for converted and nonconverted waves in anisotropic media: Geophysics, **58**, 265–276.

Shah, P. M., 1973, Use of wavefront curvature to relate seismic data with subsurface parameters: Geophysics, **38**, 812–825.

Thomsen, L., 1986, Weak elastic anisotropy: Geophysics, **51**, 1954–1966.

Tsvankin, I., 1995, Normal moveout from dipping reflectors in anisotropic media: Geophysics, **60**, 268–284.

Tsvankin, I., and Thomsen, L., 1994, Nonhyperbolic reflection moveout in anisotropic media: Geophysics, **59**, 1290–1304.

——— 1995, Inversion of reflection traveltimes for transverse isotropy: Geophysics, **60**, 1095–1107.

VerWest, B. J., 1989, Seismic migration in elliptically anisotropic media: Geophys. Prosp., **37**, 149–166.

APPENDIX A

DEPENDENCE OF NMO VELOCITY ON THE RAY PARAMETER

For the purposes of the inversion procedure, we need to recast the NMO velocity as a function of the ray parameter $p(\phi)$ (horizontal slowness) corresponding to the zero-offset reflection. The vertical (m) and horizontal (p) slownesses for P-waves in transversely isotropic media with a vertical symmetry axis (VTI) satisfy the following equation (e.g., Larner, 1993)

$$1 = 0.5\{(a_{11} + a_{44})p^2 + (a_{33} + a_{44})m^2 + \{[(a_{11} - a_{44})p^2 - (a_{33} - a_{44})m^2]^2 + 4(a_{13} + a_{44})^2 p^2 m^2\}^{1/2}\},$$

where the a_{ij} are density-normalized elastic constants.

This equation can be solved for m for a known value of the ray parameter p. If both slowness components are obtained, the phase velocity is simply

$$V(p) = \frac{1}{\sqrt{p^2 + m^2(p)}},$$

and the phase (dip) angle ϕ is given by

$$\phi = \sin^{-1}[V(p)p].$$

After the angle ϕ has been found, we can compute the derivatives of phase velocity needed in equation (1) and then obtain the P-wave NMO velocity as a function of ray parameter. The dependence $V_{\mathrm{nmo}}(p)$ can also be built parametrically by calculating V_{nmo} and p as functions of the dip ϕ.

Since phase velocity is a complicated function of the phase angle (or ray parameter) and anisotropic coefficients, it is hardly feasible to find a simple form for $V_{\mathrm{nmo}}(p)$ in general VTI media. Therefore, we consider the special cases of elliptical and weak anisotropy.

The normal-moveout velocity in elliptically anisotropic media ($\varepsilon = \delta$) can be represented as (Tsvankin, 1995)

$$V_{\mathrm{nmo}}(\phi) = \frac{V_{\mathrm{nmo}}(0)}{\cos\phi}\frac{V_P(\phi)}{V_{P0}} = \frac{V_{\mathrm{nmo}}(0)}{pV_{P0}}\tan\phi. \qquad \text{(A-1)}$$

Now we have to obtain the angle ϕ as a function of the ray parameter. The P-wave phase velocity for elliptical anisotropy, expressed through $\varepsilon = \delta$, is given by

$$V_P(\theta) = V_{P0}\sqrt{1 + 2\delta\sin^2\theta}, \qquad \text{(A-2)}$$

where θ is the phase angle measured from the symmetry axis. Then

$$p(\phi) = \frac{\sin\phi}{V_{P0}\sqrt{1 + 2\delta \sin^2\phi}}. \quad \text{(A-3)}$$

Solving equation (A-3) for the dip angle ϕ yields

$$\sin\phi = \frac{pV_{P0}}{\sqrt{1 - 2\delta p^2 V_{P0}^2}}. \quad \text{(A-4)}$$

Calculating $\tan\phi$ from equation (A-4) and taking into account that $V_{\text{nmo}}(0) = V_{P0}\sqrt{1 + 2\delta}$, we get from equation (A-1)

$$V_{\text{nmo}}(p) = \frac{V_{\text{nmo}}(0)}{\sqrt{1 - p^2 V_{\text{nmo}}^2(0)}}. \quad \text{(A-5)}$$

Therefore, for elliptical anisotropy, P-wave NMO velocity is a function of the ray parameter and zero-dip moveout velocity, with no separate dependence on the coefficient δ.

Now we carry out a similar derivation for general transverse isotropy ($\varepsilon \neq \delta$) using the weak-anisotropy approximation ($|\varepsilon| \ll 1$, $|\delta| \ll 1$). The weak-anisotropy expression for NMO velocity as a function of the dip angle ϕ was derived by Tsvankin (1995).

$$V_{\text{nmo}}(\phi) = \frac{V_P(\phi)}{\cos\phi}[1 + \delta + 2(\varepsilon - \delta)\sin^2\phi(1 + 2\cos^2\phi)]. \quad \text{(A-6)}$$

To find the dependence of normal moveout velocity on p, we have to obtain the angle ϕ as a function of the ray parameter. The P-wave phase velocity, linearized in the parameters ε and δ, is given in Thomsen (1986).

$$V_P(\theta) = V_{P0}(1 + \delta \sin^2\theta \cos^2\theta + \varepsilon \sin^4\theta). \quad \text{(A-7)}$$

The ray parameter [equation (2)] then becomes

$$p = \frac{\sin\phi}{V_{P0}(1 + \delta \sin^2\phi \cos^2\phi + \varepsilon \sin^4\phi)}. \quad \text{(A-8)}$$

After some algebra, formula (A-8) can be transformed into a quadratic equation for $\sin^2\phi$ with the solution (in the weak-anisotropy approximation)

$$\sin^2\phi = \frac{p^2 V_{P0}^2}{1 - 2\delta p^2 V_{P0}^2}[1 + 2(\varepsilon - \delta)p^4 V_{P0}^4]. \quad \text{(A-9)}$$

Substitution of the angle ϕ from equation (A-9) into (A-6) and further linearization in ε and δ leads to the following expression for the NMO velocity:

$$V_{\text{nmo}}^2(p) = \frac{V_{\text{nmo}}^2(0)}{1 - p^2 V_{\text{nmo}}^2(0)}[1 + 2(\varepsilon - \delta)f(pV_{\text{nmo}}(0))], \quad \text{(A-10)}$$

$$f = \frac{y(4y^2 - 9y + 6)}{1 - y}; \quad y \equiv p^2 V_{\text{nmo}}^2(0).$$

In the derivation of equation (A-10), we have replaced the vertical velocity V_{P0} in the anisotropic terms with $V_{\text{nmo}}(0)$ since the difference between V_{P0} and $V_{\text{nmo}}(0)$ will change only the terms quadratic in the anisotropy parameters.

It was also assumed that $y < 1$.

APPENDIX B

NMO EQUATION FOR A LAYERED MEDIUM WITH A DIPPING REFLECTOR

Here we generalize the NMO equation given in Tsvankin (1995) for layered anisotropic media with a dipping reflector. We consider a layered anisotropic model consisting of a stack of horizontal homogeneous layers above a dipping reflector (Figure B-1). It is assumed that the CMP line is perpendicular to the strike of the reflector, and the incidence (sagittal) plane coincides with a plane of symmetry in all layers.

Therefore, the kinematics of wave propagation is two-dimensional, i.e., phase and group velocity vectors do not deviate from the incidence plane. The same assumption was made in Tsvankin (1995) in the derivation of the one-layer NMO equation.

Since the medium above the reflector is laterally homogeneous, the ray parameter p (horizontal slowness) of any given ray remains constant between the reflector and the surface. In this case, it is convenient to express the short-spread moveout velocity V_{nmo} in CMP geometry as follows (Hale et al., 1992; Tsvankin, 1995):

$$V_{\text{nmo}}^2(p_0) = \lim_{x\to 0}\frac{d(x^2)}{d(t^2)} = \frac{2}{t_0}\lim_{h\to 0}\frac{dh}{dp}, \quad \text{(B-1)}$$

where $h = x/2$ is half the source-receiver offset ($h > 0$ in the down-dip direction), p_0 is the ray parameter of the zero-offset ray ($x = 0$), and t_0 is the two-way zero-offset traveltime. Note that the zero-offset ray is not necessarily perpendicular to the reflector in the presence of anisotropy; it is the phase-velocity vector corresponding to the zero-offset ray that should be normal to the reflector.

Neglecting the displacement of the reflection point on short spreads used in equation (B-1) (Tsvankin, 1995), we can represent h as

$$h = \left(\sum_{i=1}^{n} x^{(i)} - x_0\right),$$

where $x^{(i)}$ is the horizontal displacement of the ray in layer i, and x_0 is the total horizontal displacement of the zero-offset ray, between the CMP (CRP) location and the reflection point (Figure B-1). Equation (B-1) now becomes

$$V_{\text{nmo}}^2(p_0) = \frac{1}{t_0}\lim_{p\to p_0}\sum_{i=1}^{n}\frac{d(2x^{(i)})}{dp}. \quad \text{(B-2)}$$

Each component of the sum in equation (B-2) represents the squared NMO velocity in an individual layer multiplied by the corresponding zero-offset time [see equation (B-1)]. That is,

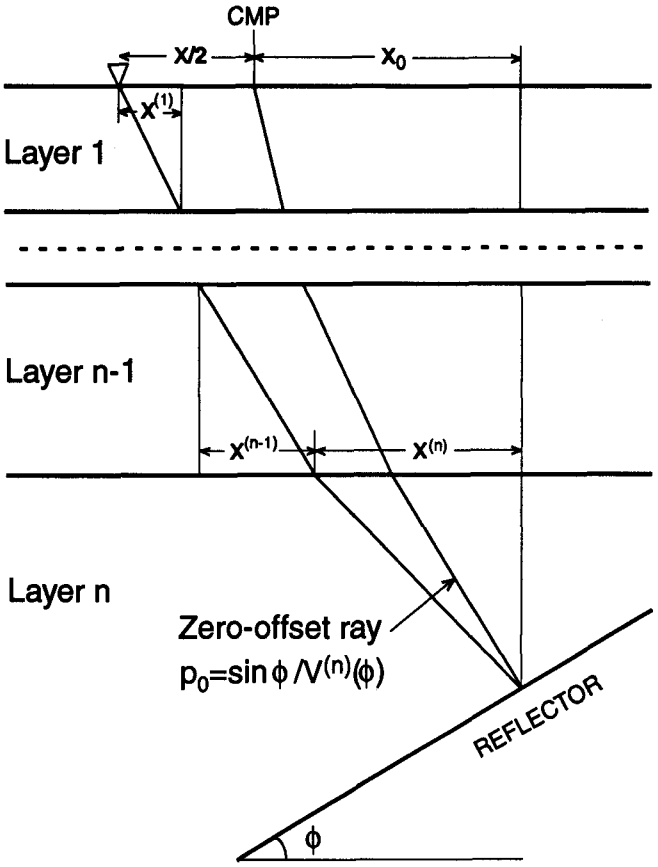

FIG. B-1. A stratified anisotropic model that includes a dipping reflector beneath a stack of horizontal homogeneous layers. It is assumed that the incidence (sagittal) plane represents the dip plane of the reflector and a symmetry plane of the medium. $V^{(n)}$ is the phase velocity in the layer immediately above the reflector.

$$\lim_{p\to p_0} \frac{d(2x^{(i)})}{dp} = t_0^{(i)}[V_{\mathrm{nmo}}^{(i)}(p_0)]^2, \tag{B-3}$$

where $t_0^{(i)}$ is the two-way traveltime along the zero-offset ray in layer i.

Tsvankin (1995) expressed $V_{\mathrm{nmo}}^{(i)}$ analytically through the phase angle $\phi^{(i)} = \sin^{-1}[p_0 V^{(i)}(p_0)]$ corresponding to the zero-offset ray, where $V^{(i)}$ is the phase velocity in layer i. In Appendix A and in the main text, we show how this NMO equation can be rewritten as a function of the ray parameter p_0.

Substituting formula (B-3) into the equation for the NMO velocity (B-2) yields

$$V_{\mathrm{nmo}}^2(p_0) = \frac{1}{t_0}\sum_{i=1}^{n} t_0^{(i)}[V_{\mathrm{nmo}}^{(i)}(p_0)]^2. \tag{B-4}$$

Equation (B-4) includes the traveltime t_0 along the ray with the ray-parameter value p_0. Below, we derive an equation for $t_0(p)$ valid for isotropy or elliptical anisotropy. For both models, the moveout is purely hyperbolic, and

$$t_0^2(p) = t_0^2(0) + \frac{x^2}{V_{\mathrm{nmo}}^2(0)}. \tag{B-5}$$

The offset x in equation (B-5) can be represented as $x = t_0 V_0 \tan\psi$ (V_0 is the vertical velocity, ψ is the group angle corresponding to the ray-parameter value p). Next, we express ψ through the phase angle θ using general relations for transverse isotropy (Thomsen, 1986) and equations (A-2) and (5):

$$\tan\psi = \tan\theta\,\frac{V_{\mathrm{nmo}}^2(0)}{V_0^2}.$$

Equation (B-5) then becomes

$$t_0^2(p) = t_0^2(0)\left(1 + \tan^2\theta\,\frac{V_{\mathrm{nmo}}^2(0)}{V_0^2}\right). \tag{B-6}$$

Using the relation between the phase angle and ray parameter for elliptical anisotropy [equation (A-4)] and equation (A-5), we find

$$t_0(p) = t_0(0)\sqrt{1 + p^2 V_{\mathrm{nmo}}^2(p)}. \tag{B-7}$$